

# Effect of Compressed CO<sub>2</sub> on the Critical Micelle Concentration and Aggregation Number of AOT Reverse Micelles in Isooctane\*\*

Jing Chen, Jianling Zhang, Buxing Han,\* Xiaoying Feng, Minqiang Hou, Wenjing Li, and Zhaofu Zhang<sup>[a]</sup>

**Abstract:** The effect of compressed CO<sub>2</sub> on the critical micelle concentration (cmc) and aggregation number of sodium bis-2-ethylhexylsulfosuccinate (AOT) reverse micelles in isooctane solution was studied by UV/Vis and fluorescence spectroscopy methods in the temperature range of 303.2–318.2 K and at different pressures or mole fractions of CO<sub>2</sub> ( $X_{\text{CO}_2}$ ). The capacity of the reverse micelles to solubilize water was also determined by direct observa-

tion. The standard Gibbs free energy ( $\Delta G^{\text{m}}$ ), standard enthalpy ( $\Delta H^{\text{m}}$ ), and standard entropy ( $\Delta S^{\text{m}}$ ) for the formation of the reverse micelles were calculated by using the cmc data determined. It was discovered that the cmc versus  $X_{\text{CO}_2}$  curve and the  $\Delta G^{\text{m}}$  versus  $X_{\text{CO}_2}$  curve for a fixed temperature have a minimum, and the aggregation

number and water-solubilization capacity of the reverse micelles reach a maximum at the  $X_{\text{CO}_2}$  value corresponding to that minimum. These results indicate that CO<sub>2</sub> at a suitable concentration favors the formation of and can stabilize AOT reverse micelles. A detailed thermodynamic study showed that the driving force for the formation of the reverse micelles is entropy.

**Keywords:** aggregation • carbon dioxide • critical micelle concentration • micelles

## Introduction

Reverse micelles or water-in-oil microemulsions are generally considered as nanometer-sized water droplets dispersed in an apolar solvent with the aid of a surfactant monolayer to form a thermodynamically stable and optically transparent solution.<sup>[1]</sup> Reverse micelles have been used in many areas, including the dissolution and extraction of hydrophiles and proteins,<sup>[2–4]</sup> chemical reactions,<sup>[5–7]</sup> the preparation of nanoparticles,<sup>[8–10]</sup> and applications in the pharmaceutical and cosmetic industries.<sup>[11–13]</sup> In addition, extensive research has been done to study the properties of reverse-micellar systems, such as the micropolarity and microviscosity of the water core, micellar size, and thermodynamics. Many techniques, such as UV/Vis spectroscopy,<sup>[14–16]</sup> FTIR spectroscopy,<sup>[17–19]</sup> fluorescence spectroscopy,<sup>[20,21]</sup> small-angle neutron scattering analysis,<sup>[22,23]</sup> small-angle X-ray scattering analy-

sis,<sup>[24,25]</sup> and microcalorimetry<sup>[26–28]</sup> have been used to characterize reverse-micellar solutions. In recent years, microemulsions with supercritical CO<sub>2</sub> as the continuous phase have been studied extensively.<sup>[29–35]</sup>

It is well known that some compressed gases, such as CO<sub>2</sub>, are quite soluble in many organic solvents and they can reduce the solvent strengths to such a degree that the solutes can be precipitated.<sup>[36–38]</sup> Our previous work showed that compressed CO<sub>2</sub> and ethylene can increase the solubilization capacity of water in sodium bis-2-ethylhexylsulfosuccinate (AOT) and Triton X-100 reverse-micellar systems at suitable pressures because the gases can insert into the interfacial region to enhance the rigidity of the interface layers and reduce the interdroplet attraction.<sup>[39–41]</sup>

The tuning and control of the properties of micellar solutions with compressed CO<sub>2</sub> is a very interesting topic. The critical micelle concentration (cmc) and aggregation number are two of the most important characteristics of reverse-micellar solutions. In this work we study the effect of compressed CO<sub>2</sub> on the cmc and aggregation number of an AOT/isooctane system, and the related thermodynamic properties of the systems in the presence of CO<sub>2</sub> are also studied. As far as we know, this is the first work about how a compressed gas affects the cmc, aggregation number, and thermodynamics of a micellar system.

[a] J. Chen, Dr. J. Zhang, Prof. Dr. B. Han, X. Feng, M. Hou, W. Li, Dr. Z. Zhang  
The Center for Molecular Sciences  
Institute of Chemistry  
Chinese Academy of Sciences, Beijing 100080 (China)  
Fax: (+86)10-6255-9373  
E-mail: Hanbx@iccas.ac.cn

[\*\*] AOT = sodium bis-2-ethylhexylsulfosuccinate.

## Results and Discussion

**Phase behavior of the solution with compressed CO<sub>2</sub>:** The reverse-micellar solution is expanded after dissolution of CO<sub>2</sub>. The volume-expansion coefficient,  $\Delta V$  ( $\Delta V = (V - V_0)/V_0$ , where  $V$  and  $V_0$  are the volumes of the CO<sub>2</sub>-saturated and CO<sub>2</sub>-free solutions), of the solution at different CO<sub>2</sub> pressures was required in the spectrum study. Figure 1a

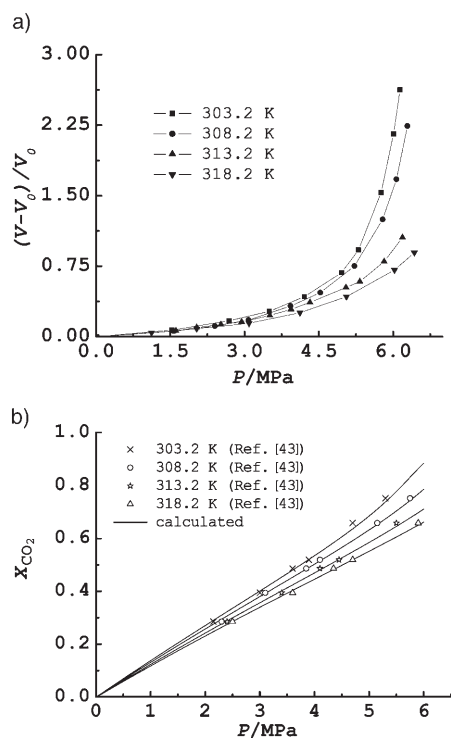


Figure 1. a) The volume-expansion coefficient,  $\Delta V$ , versus pressure curves of the AOT/isooctane solution at different temperatures ( $[AOT] = 15 \text{ mmol L}^{-1}$ ). b) Mole fractions of CO<sub>2</sub> in a CO<sub>2</sub>/isooctane mixed system at different temperatures and pressures. The lines are calculated from the Peng–Robinson equation of state. Experimental data (indicated by symbols) are taken from reference [43].

shows the  $\Delta V$  versus CO<sub>2</sub> pressure curves of AOT/isooctane solution ( $[AOT] = 15 \text{ mmol L}^{-1}$ ) at different temperatures. As expected, the  $\Delta V$  value increases with increasing pressure because the concentration of CO<sub>2</sub> in the solution is higher at higher pressure. At a given pressure, the  $\Delta V$  value decreases with increasing temperature. The AOT/isooctane micellar solution becomes cloudy as the pressure of CO<sub>2</sub> reaches the cloud-point pressure. The cloud point-pressures determined in this work for the reverse-micellar solutions at 303.2, 308.2, 313.2, and 318.2 K were 6.18, 6.50, 7.40, and 7.62 MPa, respectively. In this work, we conducted the UV and fluorescence spectroscopy experiments below 6.0 MPa to avoid the precipitation of the surfactant.

The concentrations of CO<sub>2</sub> in the CO<sub>2</sub>/isooctane mixture at different temperatures and pressures are also required in this work. It is well known that the Peng–Robinson equation of state<sup>[42]</sup> is a reliable equation to calculate this kind data.

In this work we calculated the data required with this equation and the resulting data are given in Figure 1b. The data determined by Mutelet et al.<sup>[43]</sup> are also shown in the Figure 1b. Obviously, the calculated and experimental results agree very well.

**Critical micelle concentration:** UV/Vis spectroscopy is a useful technique to determine the cmc value.<sup>[44–46]</sup> In this work, the cmc values of AOT were measured by this method. As an example, Figure 2 shows the dependence of

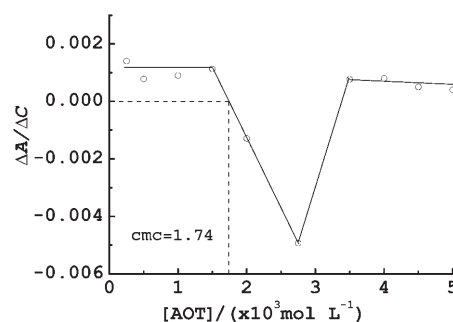


Figure 2. The plot of the differential signal of UV absorbance ( $\Delta A/\Delta C$ ) of tBP ( $5 \times 10^{-5} \text{ mol L}^{-1}$ ) in AOT/isooctane at 303.2 K and various AOT concentrations.

the differential signal of UV absorbance ( $\Delta A/\Delta C$ , where  $A$  and  $C$  are the UV absorbance and the concentration of AOT) of *tert*-butylphenol (tBP) in AOT/isooctane on the AOT concentration at 308.2 K in the absence of CO<sub>2</sub>. The shape of the curve is similar to that reported by Murali Manoj et al.<sup>[44]</sup> The plot of absorbance of tBP at maximum absorption ( $\lambda_{\text{max}}$ ) shows a discontinuous and abrupt change at the cmc value, where  $\Delta A/\Delta C$  is zero. Table 1 lists the cmc values determined under different conditions. The cmc values of AOT in CO<sub>2</sub>-free isooctane reported by other authors are also listed in the table. It can be seen that the results of this work agree reasonably with those reported by other authors.

Table 1. cmc [ $\text{mmol L}^{-1}$ ] values of AOT in isooctane at different conditions.

$X_{CO_2}$	cmc	$X_{CO_2}$	cmc
$T = 303.2 \text{ K}$		$T = 308.2 \text{ K}$	
0	1.74 (1.5 <sup>[a]</sup> )	0	1.25 (1.1 <sup>[a]</sup> )
0.14	1.36	0.13	1.06
0.40	1.06	0.37	0.87
0.53	1.37	0.50	1.02
0.68	1.56	0.63	1.12
0.88	1.67	0.78	1.2
$T = 313.2 \text{ K}$		$T = 318.2 \text{ K}$	
0	0.89	0	0.70 (0.6 <sup>[a]</sup> )
0.12	0.79	0.12	0.64
0.36	0.71	0.34	0.62
0.47	0.90	0.44	0.86
0.58	0.98	0.55	0.95
0.71	1.07	0.66	1.05

[a] The data in parentheses are those reported in reference [44].

The dependence of the cmc value of AOT on the mole fraction of CO<sub>2</sub> ( $X_{\text{CO}_2}$ ) in the solution at different temperatures is illustrated in Figure 3. The cmc value decreases with increasing temperature at a fixed  $X_{\text{CO}_2}$  value. As shown in

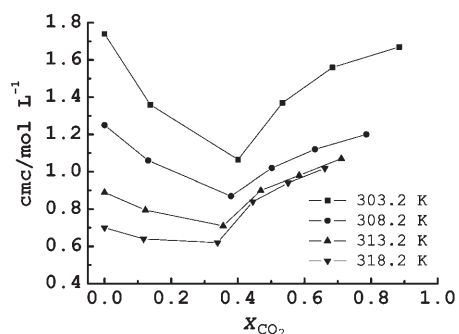


Figure 3. The dependence of the cmc value of AOT on the mole fraction of CO<sub>2</sub> ( $X_{\text{CO}_2}$ ) at different temperatures.

Figure 3, at a fixed temperature, the cmc value decreases with increasing CO<sub>2</sub> concentration at lower  $X_{\text{CO}_2}$  values and then increases with  $X_{\text{CO}_2}$  value after passing through a minimum. This means that addition of CO<sub>2</sub> is favorable to the formation of the reverse micelles in a suitable CO<sub>2</sub> concentration range. At 303.2, 308.2, 313.2, and 318.2 K, the  $X_{\text{CO}_2}$  values at which the minima occur are 0.40, 0.37, 0.36, and 0.34, respectively.

#### The effect of CO<sub>2</sub> on the stability of the reverse micelles:

The influence of CO<sub>2</sub> on the cmc value can be related to its effect on the stability of the reverse micelles. In order to study the mechanism by which CO<sub>2</sub> affects the cmc value, we studied the effect of CO<sub>2</sub> on the water solubilization of the micellar solution with an AOT concentration of 100 mmol L<sup>-1</sup>; this effect is related to the stability of the reverse micelles. Figure 4 shows the water-to-AOT molar ratio ( $w_0$ ) as a function of  $X_{\text{CO}_2}$  in the AOT/isooctane system at 303.2 K. An obvious increase of the water solubilization capacity in AOT/isooctane can be achieved with the aid of compressed CO<sub>2</sub>. In the absence of compressed CO<sub>2</sub>, phase separation occurs when the  $w_0$  value exceeds 53. At the

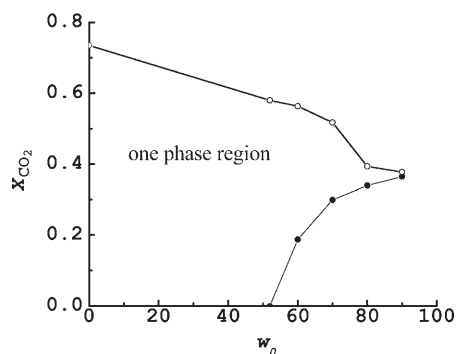


Figure 4. The  $w_0$  value as a function of the  $X_{\text{CO}_2}$  value in the AOT/isooctane system at 303.2 K ( $[\text{AOT}] = 100 \text{ mmol L}^{-1}$ ).

lower  $X_{\text{CO}_2}$  values, the solubilization capacity increases with increasing pressure. The  $X_{\text{CO}_2}$  range in which the system is single phase gradually decreases as the  $w_0$  value approaches  $w_0^{\text{max}}$  (the maximum water-to-AOT molar ratio at all the  $X_{\text{CO}_2}$  values). A further increase in CO<sub>2</sub> concentration reduces the  $w_0$  value, as demonstrated in Figure 4. The  $X_{\text{CO}_2}$  values corresponding to the  $w_0^{\text{max}}$  value at 303.2, 308.2, 313.2, and 318.2 K determined in this work are 0.38, 0.37, 0.36, and 0.34, respectively.

Figure 5 shows the dependence of the  $w_0^{\text{max}}$  value on temperature between 303.2–318.2 K. The  $w_0^{\text{max}}$  value is consider-

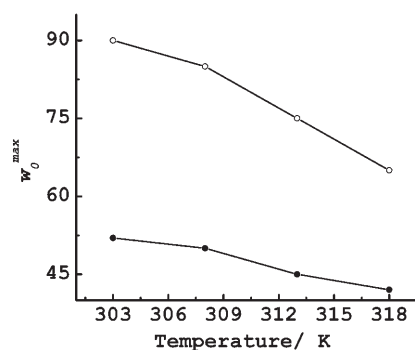


Figure 5. The dependence of the  $w_0^{\text{max}}$  value on temperature in the absence (●) and presence (○) of CO<sub>2</sub>.

ably higher in the presence of compressed CO<sub>2</sub>. This further indicates that compressed CO<sub>2</sub> can enhance the stability of the micelles. The reason is that CO<sub>2</sub> can penetrate into the interfacial film of the reverse micelles and stabilize them by increasing the rigidity of the micelle interlayer, thus reducing the attractive interaction between the droplets.<sup>[39]</sup>

Interestingly, the  $X_{\text{CO}_2}$  value corresponding to the minimum cmc point in Figure 3 is consistent with the  $X_{\text{CO}_2}$  value at which the  $w_0^{\text{max}}$  value occurs. We can deduce that CO<sub>2</sub> in the solution affects the cmc value in two opposite ways. First, it can stabilize the reverse micelles, a process that is favorable to enhancing the formation of the reverse micelles or reducing the cmc value, and second, CO<sub>2</sub> in the solvent reduces the hydrophobicity of the solvent because CO<sub>2</sub> is less hydrophobic than isooctane; the latter process is not favorable to reducing the cmc value. At the lower  $X_{\text{CO}_2}$  values the first factor is dominant, while at the higher  $X_{\text{CO}_2}$  values the second factor becomes dominant; this results in a minimum in each of the cmc versus  $X_{\text{CO}_2}$  curves.

**Aggregation number:** Fluorescence spectroscopy is a commonly used technique to study the aggregation number of micelles.<sup>[44,47–50]</sup> Many fluorescence studies of AOT/oil reverse micelles in the absence of CO<sub>2</sub> have been reported.<sup>[44,47–50]</sup> To measure the aggregation number of the AOT/isooctane system, 8-anilino-1-naphthalenesulfonic acid (ANS) is used as the probe and *N*-cetylpyridinium chloride (CPC) is used as the quencher. As an example, Figure 6a shows the dependence of the fluorescence spectra of ANS

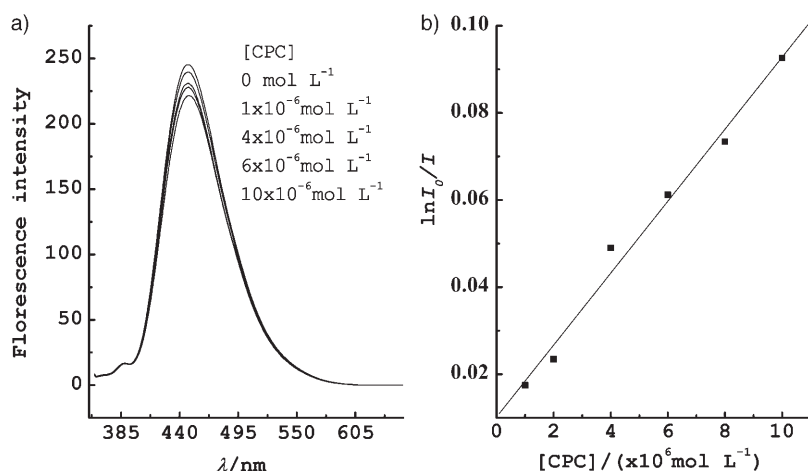


Figure 6. a) Fluorescence spectra of ANS at different CPC concentrations, [CPC], in CO<sub>2</sub>-free micellar solution. b) The corresponding ln*I*<sub>0</sub>/*I* versus [CPC] curve. *T* = 303.2 K, ([AOT] = 15 mmol L<sup>-1</sup>), [ANS] = 2 × 10<sup>-6</sup> mol L<sup>-1</sup>, λ<sub>ex</sub> = 346 nm.

on the concentration of CPC at an AOT concentration of 15 mmol L<sup>-1</sup> in CO<sub>2</sub>-free isooctane at 303.2 K. The fluorescence intensity of ANS decreases with increasing concentrations of CPC. Figure 6b presents the ln*I*<sub>0</sub>/*I* versus [CPC] curve (where *I*<sub>0</sub> and *I* are the emitted fluorescence intensities with quencher concentration of zero and a particular value, respectively) corresponding to the results in Figure 6a. The aggregation number in CO<sub>2</sub>-free reverse micelles determined by fluorescence quenching is 125, which agrees with the result reported by other authors.<sup>[44]</sup> We also determined the aggregation numbers of AOT reverse micelles in isooctane at 303.2 K and with different mole fractions of CO<sub>2</sub>; the results are listed in Table 2. It can be ob-

Table 2. The aggregation number, *N*, of the reverse micelles in the AOT/isooctane system at 303.2 K and with different mole fractions of CO<sub>2</sub>, *X*<sub>CO<sub>2</sub></sub>.

<i>X</i> <sub>CO<sub>2</sub></sub>	0	0.14	0.40	0.53	0.68
<i>N</i>	125	207	456	189	165

served that the aggregation number also has a maximum at about *X*<sub>CO<sub>2</sub></sub> = 0.40. We believe that the maximum micellar size is also related to the ability of CO<sub>2</sub> to stabilize the reverse micelles and to change the hydrophobicity and/or solvent strength of the solvent. At about *X*<sub>CO<sub>2</sub></sub> = 0.40, CO<sub>2</sub> can stabilize the reverse micelles effectively by penetrating into the interfacial region, which makes the interfacial films more rigid. Therefore, the size of the reverse micelles can be larger. The large size of the reverse micelles can partially explain the maximum solubilization capacity of water at about *X*<sub>CO<sub>2</sub></sub> = 0.40, as shown in Figure 4.

**Thermodynamics of micellization:** The thermodynamics of micellization of different surfactants in the absence of CO<sub>2</sub> have been studied extensively.<sup>[51–58]</sup> The determination of thermodynamic parameters of micellization from the cmc

value is usually based on the van't Hoff equation. In the van't Hoff method, the cmc value of a surfactant is measured at different temperatures and the energetic parameters can be evaluated by the mass action and pseudophase models.<sup>[59–61]</sup> However, the determination of thermodynamic parameters for ionic surfactants through the cmc value is more complex than that with nonionic surfactants owing to the binding of counterions to the charged micelles in the former case. It has been reported that about 90% counterions (Na<sup>+</sup> ions) are bound for AOT normal micelles.<sup>[62]</sup> In

this work, the cmc value is measured in dry reverse micelles, and it is acceptable to consider that the counterions are all bound to the AOT anions in the AOT reverse micelles. The standard free energy of micellization, Δ*G*<sup>m</sup>, can be calculated by Equation (1).<sup>[63]</sup>

$$\Delta G^m = 2RT \ln(\text{cmc}) \quad (1)$$

The standard enthalpy (Δ*H*<sup>m</sup>) and standard entropy (Δ*S*<sup>m</sup>) of micellization can be calculated from the Gibbs equation according to Equations (2) and (3).<sup>[44,59]</sup>

$$\Delta H^m = -2RT^2 d \ln(\text{cmc}) / dT \quad (2)$$

$$\Delta S^m = (\Delta H^m - \Delta G^m) / T \quad (3)$$

The thermodynamic parameters for the micelle formation at different temperatures and CO<sub>2</sub> pressures have been evaluated from Equations (1)–(3). The ln(cmc) versus temperature curves are linear at CO<sub>2</sub> pressures of 0, 1.0, and 3.0 MPa, as shown in Figure 7a, and therefore the Δ*H*<sup>m</sup> value can be easily calculated from the slope of the curves by using Equation (2). At 4.0, 5.0, and 6.0 MPa, however, the ln(cmc) versus temperature curves are not linear (Figure 7b). To evaluate the Δ*H*<sup>m</sup> value at these pressures, Equation (4), where a–d are constants, is used to correlate the data.

$$\ln(\text{cmc}) = a + bT + cT^2 + dT^3 \quad (4)$$

Figure 7b shows that Equation (4) can correlate the experimental data well. Equation (5) is obtained by differentiation of Equation (4).

$$d \ln(\text{cmc}) / dT = b + 2cT + 3dT^2 \quad (5)$$

From a combination of Equations (2) and (5), an expres-

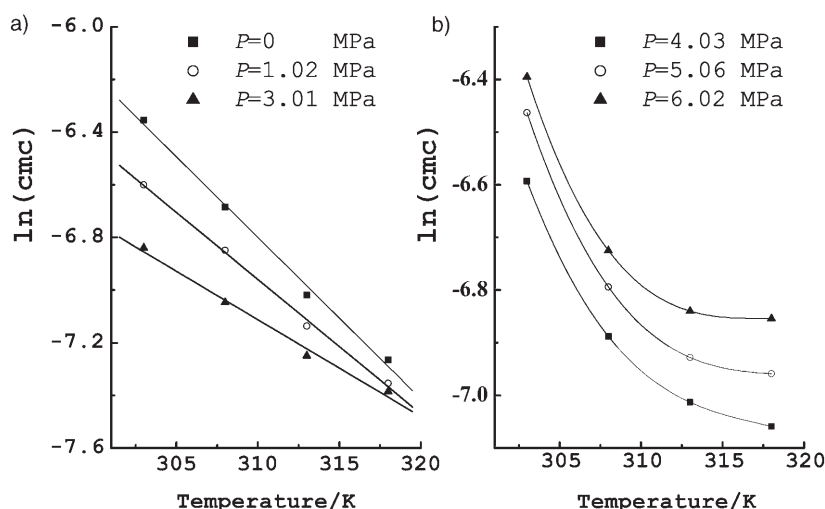


Figure 7. Plot of the  $\ln(\text{cmc})$  value against temperature for the AOT/isooctane solution at different pressures of CO<sub>2</sub>. The symbols are the experimental values and the curves are fitted results

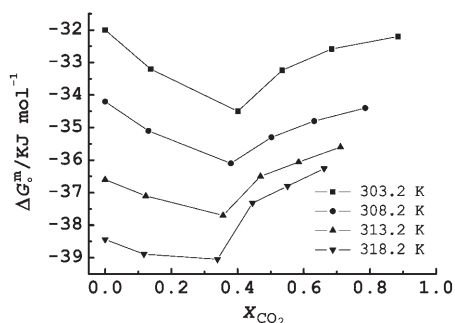


Figure 8. The dependence of the standard Gibbs free energy of micellization,  $\Delta G_m^0$ , on the mole fraction of CO<sub>2</sub>,  $X_{\text{CO}_2}$ , at different temperatures.

sion of the  $\Delta H_m^0$  value can be obtained [Eq. (6)].

$$\Delta H_m^0 = -2RT^2(b+2cT+3dT^2) \quad (6)$$

Figure 8 shows the  $\Delta G_m^0$  value as a function of  $X_{\text{CO}_2}$  at different temperatures. The  $\Delta G_m^0$  value is negative under all the conditions and has a minimum in each curve, thereby indicating that the formation of AOT micelles in isooctane and in CO<sub>2</sub>/isooctane is spontaneous and thermodynamically favored, especially at the  $X_{\text{CO}_2}$  values where the minima occur. In other words, addition of CO<sub>2</sub> at suitable

$X_{\text{CO}_2}$  values is favorable to the formation of the reverse micelles. Furthermore, as expected, the  $X_{\text{CO}_2}$  value with the minimum  $\Delta G_m^0$  value is coincident with the one where the minimum cmc value is observed.

Figure 9 shows the dependence of  $\Delta H_m^0$  and  $T\Delta S_m^0$  on the  $X_{\text{CO}_2}$  value at different temperatures. The  $\Delta H_m^0$  value is positive, which indicates that formation of the reverse micelles is endothermic process. Thermodynamically, the process to form the reverse micelles can be divided into two steps. First, the removal of solvent molecules from the vicinity of the AOT molecules, a process that

is associated with a positive enthalpy change.<sup>[28]</sup> Second, AOT molecules aggregate to form the reverse micelles; this process gives a negative contribution to the enthalpy change.<sup>[28]</sup> The positive  $\Delta H_m^0$  value suggests that the first step dominates the micellization energetically.

The positive  $\Delta S_m^0$  value indicates that the system becomes more disordered during the micellization process in the solvent. Similar to the situation with the  $\Delta H_m^0$  value, the  $\Delta S_m^0$  value can also be divided into two parts. The entropy change of removing solvent molecules from the vicinity of the AOT molecules is associated with a positive entropy change,<sup>[63]</sup> while the aggregation of the AOT molecules to form the reverse micelles gives a negative contribution to

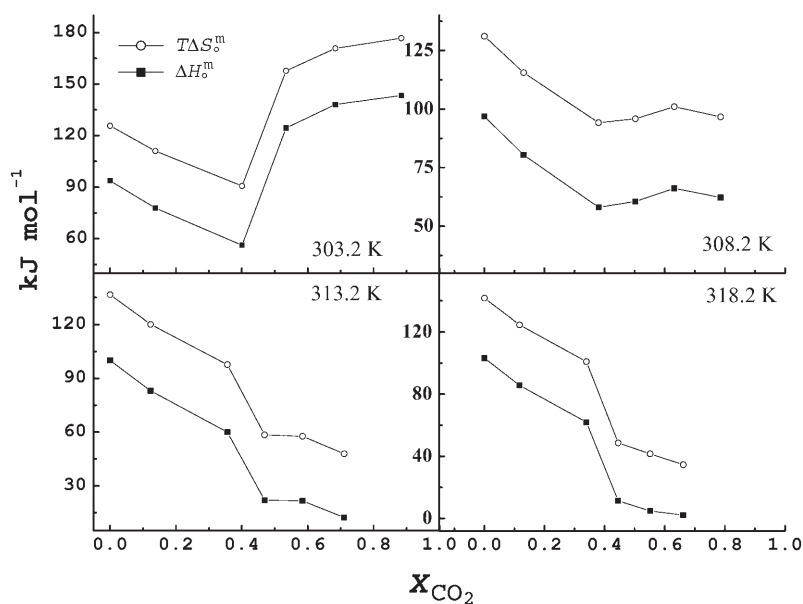


Figure 9. The thermodynamic parameters,  $\Delta H_m^0$  and  $\Delta S_m^0$ , for micellization of AOT as a function of the mole fraction of CO<sub>2</sub>,  $X_{\text{CO}_2}$ , at different temperatures.

the entropy change. The positive  $\Delta S^m$  value suggests that the former is dominant. According to the idea of enthalpy–entropy compensation,<sup>[64–67]</sup> the contribution of the enthalpy ( $\Delta H^m$ ) for the Gibbs free energy is small compared to the entropy term ( $T\Delta S^m$ ), that is, the entropy change is the major driving force for the formation of the reverse micelles.

It can be observed that, at 313.2 K and 318.2 K, the  $\Delta H^m$  and  $\Delta S^m$  values decrease continuously with increasing  $\text{CO}_2$  concentration over the entire  $X_{\text{CO}_2}$  range. As discussed above, the  $\Delta H^m$  and  $\Delta S^m$  values can be supposed to be the contribution of two processes, namely the removal of solvent molecules from the vicinity of the AOT molecules and aggregation of the AOT molecules to form the reverse micelles. The size of  $\text{CO}_2$  is much smaller than that of isooctane, and it can insert into the tail region of the reverse micelles to stabilize the micelles. This means that it is not necessary to remove all of the solvent molecules in the first step. Therefore, in the presence of  $\text{CO}_2$ , the first step is less endothermic and its contribution to entropy change is smaller than is the case without  $\text{CO}_2$ . More  $\text{CO}_2$  molecules insert into the interfacial films at the higher  $\text{CO}_2$  concentrations, and the  $\Delta H^m$  and  $\Delta S^m$  values decrease with increasing  $\text{CO}_2$  concentration. This can also be considered in another way. It can be supposed that all of the solvent molecules are removed in the first step, while, after the aggregation of AOT molecules in the second step, some  $\text{CO}_2$  molecules insert into the interfacial films; this is an exothermic process and the entropy is reduced because  $\text{CO}_2$  molecules are bound to the AOT molecules.

At 303.2 K, an increase in  $\text{CO}_2$  concentration results in a decrease in the  $\Delta H^m$  and  $\Delta S^m$  values at the lower  $X_{\text{CO}_2}$  values and an increase with increasing  $X_{\text{CO}_2}$  values at the higher  $\text{CO}_2$  concentrations, as shown in Figure 9. It is very difficult to give an exact explanation for this interesting phenomenon. This may be partially related with the special properties of near-critical fluids. It is known that near-critical fluids can form clusters with solutes in the critical region, which is often called local-density and/or local-composition enhancement.<sup>[68,69]</sup> The clustering between solvents and solutes is an exothermic process.<sup>[70,71]</sup> Therefore, with an increasing content of  $\text{CO}_2$  in the solution, the solvent approaches its critical point, and the clustering of the solvent and AOT becomes more significant or the local density of the solvent around the AOT monomers can be considerably higher than that in the bulk. Thus, in the first step (removal of solvent molecules from the vicinity of the AOT molecules), a large amount of solvent molecules enters the continuous phase and the process is more endothermic, and therefore the contribution to  $\Delta S^m$  is large. The clustering is more significant with a higher content of  $\text{CO}_2$  and the  $\Delta H^m$  and  $\Delta S^m$  values increase with the increasing content of  $\text{CO}_2$ . The content of  $\text{CO}_2$  in the solvent at the higher temperatures is much smaller (Figure 1) and the solution exhibits mainly the properties of conventional liquids, so the  $\Delta H^m$  and  $\Delta S^m$  values decrease continuously as pressure rises.

It should be mentioned that the effect of  $\text{CO}_2$  on the  $\Delta H^m$  and  $\Delta S^m$  values is more complex than that discussed above. For example, the interaction between the  $\text{CO}_2$  and AOT may be considerably different from that between the isooctane and AOT.

## Conclusion

In this work we studied the effect of  $\text{CO}_2$  on the cmc value of AOT in isooctane, the aggregation number of the reverse micelles, the ability of the reverse micelles to solubilize water, and the thermodynamic properties of the micellization at different temperature and  $X_{\text{CO}_2}$  values. It was discovered that the cmc value decreases with increasing  $X_{\text{CO}_2}$  values in the lower  $X_{\text{CO}_2}$  ranges, but it increases with the  $X_{\text{CO}_2}$  value at higher  $\text{CO}_2$  concentrations. The  $\Delta G^m$  value is negative and shows a minimum in each  $\Delta G^m$  versus  $X_{\text{CO}_2}$  curve, a result indicating that the micellization of AOT in isooctane is thermodynamically favored and spontaneous, especially at suitable  $\text{CO}_2$  concentrations. The aggregation number of the reverse micelles increases with increasing  $X_{\text{CO}_2}$  values in the lower  $\text{CO}_2$  concentration range and decreases with  $\text{CO}_2$  concentration at higher  $\text{CO}_2$  concentrations. The ability of the reverse micelles to solubilize water also shows a maximum at a suitable  $\text{CO}_2$  concentration. The changes of cmc value and  $\Delta G^m$  upon addition of  $\text{CO}_2$  indicate that  $\text{CO}_2$  at a suitable concentration favors the micellization of AOT in the solvent. The effect of  $\text{CO}_2$  on the aggregation number and the solubilization ability of the reverse micelles suggests that  $\text{CO}_2$  at a suitable concentration can stabilize the reverse micelles.  $\text{CO}_2$  can insert into the interlayer region of the reverse micelles, increase the rigidity of the interfacial film, and reduce the micelle–micelle interaction. Therefore,  $\text{CO}_2$  at a suitable concentration can enhance the stability of the reverse micelles and reduce the Gibbs free energy of micellization. The  $\Delta S^m$  and  $\Delta H^m$  values are positive, a result demonstrating that the micellization process is entropy driven.

## Experimental Section

**Materials:**  $\text{CO}_2$  (>99.995% purity) was provided by Beijing Analytical Instrument Factory. The surfactant AOT (99% purity) was purchased from Sigma. In this work, the surfactant AOT was dried under vacuum at 50°C until the weight was independent of drying time and was then stored in a desiccator. The sample was dried again under vacuum for two hours before use. The isooctane (analytical grade) was supplied by Beijing Chemical Plant. The hemi-Mg salt of ANS and the CPC were purchased from Aldrich. tBP (analytical grade) was provided by Shanghai Chemical Agent Company.

**Phase behavior of the solution in the presence of compressed  $\text{CO}_2$ :** The AOT/isooctane solutions were prepared by adding suitable amounts of AOT into the isooctane solution. A transparent solution was obtained after shaking the solution for several minutes. The phase behavior of the solution in the presence of  $\text{CO}_2$  was investigated with the apparatus used previously.<sup>[72]</sup> A HAAKE D3 digital controller was used to control the temperature of the water bath; the accuracy of the temperature measure-

ment was  $\pm 0.1^\circ\text{C}$ . The pressure gauge used was composed of a pressure transducer (FOXBORO/ICT, Model 93) and an indicator, which was accurate to  $\pm 0.025\text{MPa}$  in the pressure range of 0–20 MPa. In the experiment, a suitable amount of solution was added into the viewing cell. After thermal equilibrium had been reached, CO<sub>2</sub> was charged into the cell until a suitable pressure was reached. A magnetic stirrer was used to enhance the mixing of CO<sub>2</sub> and the solution. The pressure and the volume were recorded under equilibrium conditions. More CO<sub>2</sub> was added and the volume of the liquid phase at another pressure was determined. The volume-expansion coefficient was calculated on the basis of the liquid volumes before and after the dissolution of CO<sub>2</sub>. The solution became cloudy once the pressure was high enough due to the antisolvent effect of CO<sub>2</sub>; this pressure was defined as the cloud-point pressure.

**Determination of water solubilization:** The experiments were based on the fact that the solution was clear and transparent if the water was completely solubilized; otherwise the solution was hazy or milky.<sup>[73,74]</sup> The apparatus and procedures were similar to those reported previously,<sup>[75]</sup> which were used to study other systems. The apparatus consisted mainly of a high-pressure viewing cell, a constant-temperature water bath, a high-pressure syringe pump (DB-80), a pressure gauge, a magnetic stirrer, and a gas cylinder. The temperature of the water bath was controlled by a HAAKE D3 temperature controller. In a typical experiment, the air in the viewing cell was replaced by CO<sub>2</sub>. The solution of AOT in isooctane (5 mL) and the desired amount of double-distilled water were loaded into the high-pressure viewing cell. The cell was placed into the constant-temperature water bath. After thermal equilibrium had been reached, the stirrer was started. At this point, the solution was hazy and milky. CO<sub>2</sub> was charged into the cell slowly until the hazy and milky liquid solution became transparent and completely clear, which was an indication of the solubilization of all of the water.<sup>[73–75]</sup>

**Determination of the cmc value:** The cmc value of AOT/isooctane reverse micelles was studied with a UV spectrophotometer (TU-1201) and tBP was used as an external probe.<sup>[44]</sup> The high-pressure temperature-controlled UV sample cell was the same as that used previously.<sup>[72]</sup> The optical path length and the volume of the sample cell were 1.12 cm and 1.64 mL, respectively. In a typical experiment, desired amounts of the tBP/isooctane and AOT/isooctane solutions were loaded into the sample cell and then the cell was charged with CO<sub>2</sub>, which made the cell full. The concentration of the probe was kept at  $5 \times 10^{-5}\text{molL}^{-1}$  after the solution was expanded by CO<sub>2</sub>, that is, the concentration of the probe was the same for all experiments. The differential signal of  $\Delta A/\Delta C$  (where  $A$  and  $C$  stand for the UV absorbance and concentration of AOT, respectively) was plotted against the AOT concentration for determination of the cmc values.

**Determination of aggregation number:** Fluorescence techniques were used to determine the aggregation number of the AOT/isooctane reverse micelles, and the experiments were performed by using a Hitachi F-2500 spectrofluorometer. The high-pressure fluorescence cell was similar to that used previously.<sup>[21]</sup> ANS was used as the external fluorescence probe and CPC was employed as the quencher.<sup>[44]</sup> The excitation wavelength was 346 nm, and the fluorescence emission was measured at 455 nm. In the experiment, a suitable amount of ANS-containing reverse-micellar solution and CPC-containing reverse-micellar solution were charged into the cell. The temperature of the cell was maintained at 303.2 K. The sample cell was charged with CO<sub>2</sub> until it was full. The fluorescence spectrum of the solution was recorded. The concentrations of AOT and ANS were  $15\text{mmolL}^{-1}$  and  $2 \times 10^{-6}\text{molL}^{-1}$  respectively, after the solution was expanded by CO<sub>2</sub>. This technique assumes that the number of both the probe and the quencher molecules per micelle obeys Poisson's distribution, which leads to Equation (7),<sup>[44]</sup> where  $I_0$  and  $I$  are the emitted fluorescence intensities with quencher concentration of zero and  $[Q]$ , respectively,  $N$  is the mean surfactant aggregation number, and  $C_s$  is the total AOT concentration.

$$\ln I_0/I = N[Q]/(C_s - \text{cmc}) \quad (7)$$

The aggregation number can be calculated from the slope of the plot of  $\ln(I_0/I)$  against the initial  $[Q]$  at a fixed  $C_s$ .

## Acknowledgements

The authors are grateful to the National Natural Science Foundation of China (grant no.: 20403021) and the Ministry of Science and Technology of China (grant no.: 2005cb221301) for financial support.

- [1] L. M. Nazario, T. A. Hatton, J. P. S. G. Crespo, *Langmuir* **1996**, *12*, 6326.
- [2] W. Y. Chen, Y. W. Lee, S. C. Lin, C. W. Ho, *Biotechnol. Prog.* **2002**, *18*, 1443.
- [3] A. Shioi, M. Harada, H. Takahashi, M. Adachi, *Langmuir* **1997**, *13*, 609.
- [4] K. S. Freeman, T. T. Tang, R. D. E. Shah, D. J. Kiserow, L. B. McGown, *J. Phys. Chem. B* **2000**, *104*, 9312.
- [5] A. Chive, B. Delfort, M. Born, L. Barre, Y. Chevalier, R. Gallo, *Langmuir* **1998**, *14*, 5355.
- [6] I. M. Cuccovia, L. G. Dias, F. A. Maximiano, H. Chaimovich, *Langmuir* **2001**, *17*, 1060.
- [7] A. Mallardi, G. Palazzo, G. Venturoli, *J. Phys. Chem. B* **1997**, *101*, 7850.
- [8] C. R. Vestal, Z. J. Zhang, *Chem. Mater.* **2002**, *14*, 3817.
- [9] J. L. Zhang, B. X. Han, J. C. Liu, X. G. Zhang, Z. M. Liu, J. He, *Chem. Commun.* **2001**, 2724.
- [10] M. L. Wu, D. H. Chen, T. C. Huang, *Langmuir* **2001**, *17*, 3877.
- [11] D. Salom, B. R. Hill, J. D. Lear, W. F. DeGrado, *Biochemistry* **2000**, *39*, 14160.
- [12] C. A. Rosslee, N. L. Abbott, *Anal. Chem.* **2001**, *73*, 4808.
- [13] Y. Orihara, A. Matsumura, Y. Saito, N. Ogawa, T. Saji, A. Yamaguchi, H. Sakai, M. Abe, *Langmuir* **2001**, *17*, 6072.
- [14] A. A. A. Fattah, M. E. Kelany, F. A. Rehim, A. A. E. Miligy, *J. Photochem. Photobiol. A* **1997**, *110*, 291.
- [15] K. L. Toews, M. S. Robert, C. M. Wai, N. G. Smart, *Anal. Chem.* **1995**, *67*, 4040.
- [16] D. X. Liu, J. L. Zhang, B. X. Han, J. F. Fan, T. C. Mu, Z. M. Liu, W. Z. Wu, J. Chen, *J. Chem. Phys.* **2003**, *119*, 4873.
- [17] P. D. Moran, G. A. Bowmaker, R. P. Cooney, J. R. Bartlett, J. L. Woolfrey, *Langmuir* **1995**, *11*, 738.
- [18] M. B. Tamsamani, M. Maec, I. El Hassani, H. D. Hurwitz, *J. Phys. Chem. B* **1998**, *102*, 3335.
- [19] T. K. Jain, M. Varshney, A. Maitra, *J. Phys. Chem.* **1989**, *93*, 7409.
- [20] J. D. Jordan, R. A. Dunbar, F. V. Bright, *Anal. Chem.* **1995**, *67*, 2436.
- [21] D. X. Liu, J. L. Zhang, J. F. Fan, B. X. Han, J. Chen, *J. Phys. Chem. B* **2004**, *108*, 2851.
- [22] J. B. McClain, D. E. Betts, D. A. Canelas, E. T. Samulski, J. M. Desimone, J. D. Londono, H. D. Cochran, G. D. Wignall, D. Chillura-Martino, R. Triolo, *Science* **1996**, *274*, 2049.
- [23] A. Bumajdad, J. Eastoe, R. K. Heenan, *Langmuir* **2003**, *19*, 7219.
- [24] M. Hirai, R. Kawai-Hirai, M. Sanada, H. Iwase, S. Mitsuya, *J. Phys. Chem. B* **1999**, *103*, 9658.
- [25] M. Hirai, R. Kawai-Hirai, S. Yabuki, T. Takizawa, T. Hirai, K. Kobayashi, Y. Amemiya, M. Oya, *J. Phys. Chem.* **1995**, *99*, 6652.
- [26] M. L. Das, P. K. Bhattacharya, S. P. Moulik, A. R. Das, *Langmuir* **1992**, *8*, 2135.
- [27] P. K. Jana, S. P. Moulik, *J. Phys. Chem.* **1991**, *95*, 9525.
- [28] K. Mukherjee, S. P. Moulik, D. C. Mukherjee, *Langmuir* **1993**, *9*, 1727.
- [29] T. A. Hoefling, R. M. Enick, E. J. Beckman, *J. Phys. Chem.* **1991**, *95*, 7127.
- [30] S. R. P. Da Rocha, K. P. Johnston, *Langmuir* **2000**, *16*, 3690.
- [31] J. Eastoe, A. Paul, A. Downer, *Langmuir* **2002**, *18*, 3014.
- [32] B. Xu, G. W. Lynn, J. Guo, Y. B. Melnichenko, G. D. Wignall, J. B. McClain, J. M. DeSimone, C. S. Johnson, Jr., *J. Phys. Chem. B* **2005**, *109*, 10261.
- [33] M. Ji, X. Y. Chen, C. M. Wai, J. L. Fulton, *J. Am. Chem. Soc.* **1999**, *121*, 2631.
- [34] X. Fan, V. K. Potluri, M. C. McLeod, Y. Wang, J. C. Liu, R. M. Enick, A. D. Hamilton, C. B. Roberts, J. K. Johnson, E. J. Beckman, *J. Am. Chem. Soc.* **2005**, *127*, 11754.

- [35] J. C. Liu, P. Raveendran, Z. Shervani, Y. Ikushima, Y. Hakuta, *Chem. Eur. J.* **2005**, *11*, 1854.
- [36] C. A. Eckert, L. K. Barbara, P. G. Debenedetti, *Nature* **1996**, *383*, 313.
- [37] S. Mawson, K. P. Johnson, D. E. Betts, J. B. McClain, J. M. DeSimone, *Macromolecules* **1997**, *30*, 71.
- [38] J. L. Zhang, B. X. Han, J. C. Liu, X. G. Zhang, J. He, Z. M. Liu, T. Jiang, G. Y. Yang, *Chem. Eur. J.* **2002**, *8*, 3879.
- [39] D. Shen, R. Zhang, B. X. Han, Y. Dong, W. Z. Wu, J. L. Zhang, J. C. Li, T. Jiang, Z. M. Liu, *Chem. Eur. J.* **2004**, *10*, 398.
- [40] D. Shen, B. X. Han, Y. Dong, W. Z. Wu, J. W. Chen, J. L. Zhang, *Chem. Eur. J.* **2005**, *11*, 1228.
- [41] D. Shen, B. X. Han, Y. Dong, J. W. Chen, T. C. Mu, W. Z. Wu, J. L. Zhang, *J. Phys. Chem. B* **2005**, *109*, 5796.
- [42] D. Y. Peng, D. B. Robinson, *Ind. Eng. Chem. Fundam.* **1976**, *15*, 59.
- [43] F. Mutelet, S. Vitu, R. Privat, J. Jaubert, *Fluid Phase Equilib.* **2005**, *238*, 157.
- [44] K. Murali Manoj, R. Jayakumar, S. K. Rakshit, *Langmuir* **1996**, *12*, 4068.
- [45] R. Jayakumar, A. B. Mandal, P. T. Manoharan, *J. Chem. Soc. Chem. Commun.* **1993**, 853.
- [46] R. Jayakumar, R. G. Jeevan, A. B. Mandal, P. T. Manoharan, *J. Chem. Soc. Faraday Trans.* **1994**, 2725.
- [47] A. Murphy, G. Taggart, *Colloids Surf. A* **2002**, *205*, 237.
- [48] S. P. Moulik, M. E. Haque, P. K. Jana, A. R. Das, *J. Phys. Chem.* **1996**, *100*, 701.
- [49] S. C. Bhattacharya, H. T. Das, S. P. Moulik, *J. Photochem. Photobiol. A* **1993**, *71*, 257.
- [50] N. J. Turro, A. Yekta, *J. Am. Chem. Soc.* **1978**, *100*, 5951.
- [51] S. K. Hait, S. P. Moulik, R. Palepu, *Langmuir* **2002**, *18*, 2471.
- [52] S. P. Moulik, G. C. De, B. B. Bhowmik, A. K. Panda, *J. Phys. Chem.* **1995**, *99*, 8222.
- [53] G. C. Kreshech, *J. Phys. Chem. B* **1998**, *102*, 6595.
- [54] A. Shiloach, D. Blankschtein, *Langmuir* **1998**, *14*, 4105.
- [55] A. Goto, S. Harada, T. Fujita, Y. Miwa, H. Yoshioka, H. Kishimoto, *Langmuir* **1993**, *9*, 86.
- [56] P. Majhi, A. Blume, *Langmuir* **2001**, *17*, 3844.
- [57] W. Blokzijl, J. B. F. V. Engberts, *Angew. Chem.* **1993**, *105*, 1610; *Angew. Chem. Int. Ed. Engl.* **1993**, *32*, 1545.
- [58] G. Onori, A. Santucci, *J. Phys. Chem. B* **1997**, *101*, 4662.
- [59] A. Chatterjee, S. P. Moulik, S. K. Sanyal, B. K. Mishra, P. M. Puri, *J. Phys. Chem. B* **2001**, *105*, 12823.
- [60] S. P. Moulik, *Current Sci.* **1996**, *71*, 368.
- [61] G. Sugihara, P. Mukerjee, *J. Phys. Chem.* **1981**, *85*, 1612.
- [62] K. Mukherjee, D. C. Mukherjee, S. P. Moulik, *J. Phys. Chem.* **1994**, *98*, 4713.
- [63] P. R. Majhi, S. P. Moulik, *J. Phys. Chem. B* **1999**, *103*, 5977.
- [64] S. Paula, W. Sus, J. Tuchtenhagen, A. Blume, *J. Phys. Chem.* **1995**, *99*, 11742.
- [65] B. Lee, *Biopolymers* **1991**, *31*, 993.
- [66] B. Lee, *Biophys. Chem.* **1994**, *51*, 271.
- [67] B. Madau, B. Lee, *Biophys. Chem.* **1994**, *51*, 279.
- [68] P. B. Baulbuena, K. P. Johnston, P. J. Rossky, *J. Am. Chem. Soc.* **1994**, *116*, 2689.
- [69] J. F. Brennecke, J. E. Chateaufneuf, *Chem. Rev.* **1999**, *99*, 433.
- [70] X. G. Zhang, B. X. Han, Z. S. Hou, J. L. Zhang, Z. M. Liu, T. Jiang, J. He, H. P. Li, *Chem. Eur. J.* **2002**, *8*, 5107.
- [71] T. C. Mu, X. G. Zhang, Z. M. Liu, B. X. Han, Z. H. Li, T. Jiang, J. He, G. Y. Yang, *Chem. Eur. J.* **2004**, *10*, 371.
- [72] H. F. Zhang, J. Lu, B. X. Han, *J. Supercrit. Fluids* **2001**, *20*, 65.
- [73] P. Alexandridis, K. Andersson, *J. Colloid Interface Sci.* **1997**, *194*, 166.
- [74] P. Alexandridis, K. Andersson, *J. Phys. Chem. A* **1997**, *101*, 8103.
- [75] R. Zhang, J. Liu, J. He, B. X. Han, *Macromolecules* **2002**, *35*, 7869.

Received: December 20, 2005

Revised: April 21, 2006

Published online: July 24, 2006